Spectroscopic and Spectropolarimetric Observations of V838 Mon

John P. Wisniewski[1], Nancy D. Morrison[1], Karen S. Bjorkman[1], Anatoly S.Miroshnichenko[1] ,

Amanda C. Gault[1], Jennifer L. Hoffman[2,3], Marilyn R. Meade[4], & Jason M. Nett[4]

ABSTRACT

The spectroscopic and spectropolarimetric variability of the peculiar variable V838 Monocerotis during the brighter phases of its multiple outbursts in 2002 is presented. Significant line profile variability of Hα and Si II 6347.10Å & 6371.36Å occurred in spectra obtained between 2002 February 5 and 2002 March 14, and a unique secondary absorption component was observed near the end of this time period. Our observations also suggest that multiple shifts in ionization states occurred during the outbursts. Spectropolarimetric observations reveal that V838 Mon exhibited both intrinsic and interstellar polarization components during the initial stages of the second outburst, indicating the presence of an asymmetric geometry; however, the intrinsic component had significantly declined by February 14. We determine the interstellar polarization to be $P_{max} = 2.746 \pm 0.011\%, \quad \lambda_{max} = 5790 \pm 37\AA, PA = 153.43 \pm 0.12°,$ and we find the integrated intrinsic V band polarization on February 5 to be P = 0.983± 0.012% at a position angle of 127.0±0.5°. The implications of these observations for the nature of V838 Monocerotis, its distance, and its ejecta are discussed.

Subject headings: circumstellar matter---stars: individual (V838-Mon)---techniques: polarimetric----techniques: spectroscopic

---

[1]Ritter Observatory, MS #113, Department of Physics and Astronomy, University of Toledo, Toledo, OH 43606-3390 USA, jwisnie@physics.utoledo.edu, nmorris2@uoft02.utoledo.edu, karen@physics.utoledo.edu, anatoly@physics.utoledo.edu, agault@utphya.panet.utoledo.edu

[2]Department of Astronomy, University of Wisconsin-Madison, 475 N. Charter St., Madison, WI 53706

[3]Department of Physics and Astronomy MS-108, Rice University, 6100 Main Street, Houston, TX 77005, jhoffman@rice.edu

[4]Space Astronomy Lab, University of Wisconsin-Madison, 1150 University Avenue, Madison, WI 53706, meade@sal.wisc.edu, jnett@sal.wisc.edu

1. Introduction

Brown et al. (2002) reported the discovery of a possible nova, later to be designated V838 Monocerotis, on 2002 January 6.6. Prior to outburst, V838 Mon was a hot blue star, whose B band brightness was stable at 15.85 ± 0.4 from 1949-1994 (Goranskii et al. 2002). Munari et al. (2002a) noted that V838 Mon was not detected in prior Hα emission-line surveys. A spectrum obtained on January 26 showed numerous neutral metal and s-process lines, and resembled that of a heavily reddened K-type giant (Zwitter & Munari 2002).

V838 Monocerotis underwent a second major photometric outburst in early February 2002, changing from V=10.708 on February 1.86 to V=8.024 on February 2.91 (Kimeswenger et al. 2002a), and reaching a maximum brightness of 6.66 in V on February 6 (Goranskii et al. 2002). Spectra obtained during and immediately following this outburst (Iijima & Della Valle 2002; Morrison et al. 2002) revealed the emergence of various ionized metal lines. Kaeufl et al. (2002) estimated a blackbody continuum temperature of 4500 K to be present on February 9, and Henden et al. (2002) found that a light echo had developed around V838 Mon on February 17. IRAS source 07015-0346 has been associated with the location of V838 Mon (Kato et al. 2002), leading to the suggestion that this IR emission is from the dust causing the light echoes (Kimeswenger et al. 2002b).

A third, less intense outburst occurred in early March 2002 (Kimeswenger et al. 2002b; Munari et al. 2002a). By April 16, V838 Mon's spectrum had evolved such that it resembled an M5 giant (Rauch et al. 2002) , with strong TiO molecular bands and a temperature of ∼3000 K. Banerjee & Ashok (2002) detected TiI emission lines from near infrared spectroscopy, peaking in strength on May 2, and argued that this emission arose from circumstellar ejecta. They used the strengths of these TiI lines to estimate the mass of V838 Mon's ejected envelope to be 10^{-7} to 10^{-5} $M_{\odot}$.

By October 2.17, spectroscopic observations suggested that V838 Mon had evolved into a "later than M10 III" type star (Desidera & Munari 2002). Desidera & Munari (2002) also detected a weak blue continuum, suggesting the presence of a binary companion. Followup spectroscopy (Wagner & Starrfield 2002; Munari et al. 2002c) confirmed this detection, and Munari et al. (2002c) suggested that the companion was a B3 V type star. The unique, complex evolution of V838 Monocerotis has led Munari et al. (2002a) to suggest that this object represents a new class of objects, "stars erupting into cool supergiants (SECS)".

In this paper, we report the spectroscopic and spectropolarimetric properties of V838 Monocerotis following its second and third photometric outbursts. In section 2, we outline our observational data. We detail the equivalent width and line profile variability of selected spectral lines in section 3.1. Our spectropolarimetric data, most notably the detection of

an intrinsic polarization component, are discussed in section 3.2. We address the distance to V838 Mon in section 3.3. Finally, in section 4, we discuss the implications of these observations for future studies of this unique object.

2. Observations

We obtained spectroscopic observations of V838 Monocerotis with the Ritter Observatory 1m reflector, using a fiber-fed echelle spectrograph. The fiber used for these observations has a diameter of 200 μm, which corresponds to roughly $5''$ on the sky. Nine non-adjacent orders of width 70 Å were observed in the range 5285 -6595 Å. Data were recorded on a 1200 x 800 Wright Instruments Ltd. CCD, with 22.5 x 22.5 μm pixels. With $R \equiv \lambda/\Delta\lambda \simeq 26,000$, the spectral resolution element, $\Delta\lambda$, is about 4.2 pixels owing to a widened entrance slit. Observations were reduced with IRAF[5] using standard techniques. Further details about the reduction of Ritter data can be found in Morrison et al. (1997). Unless otherwise noted, all data were shifted to the heliocentric rest frame and continuum normalized.

We obtained spectropolarimetric observations of V838 Mon with the University of Wisconsin's HPOL spectropolarimeter, which is the dedicated instrument on the 0.9m Pine Bluff Observatory (PBO) telescope. These data were recorded with a 400 x 1200 pixel CCD camera, covering the wavelength range of 3200 -10500Å, with a spectral resolution of 7Å below 6000Å and 10Å above this point (Nordsieck & Harris 1996). Observations were made with dual 6 x 12 arc-second apertures, with the 6 arc-second slit aligned E-W and the 12 arc-second decker aligned N-S on the sky. The two apertures allow simultaneous star and sky data to be recorded, providing a reliable means for subtraction of background sky polarization and hence allowing accurate observations to be made even in non-photometric skies. We processed these data using REDUCE, a spectropolarimetric software package developed by the University of Wisconsin-Madison (Wolff et al. 1996). Further details about HPOL and REDUCE may be found in Nook (1990) and Harries et al. (2000) . Instrumental polarization is monitored on a weekly to monthly basis at PBO via observations of polarized and unpolarized standard stars, and over its 13 year existence, HPOL has proven to be a very stable instrument. We have corrected our data for instrumental effects to an absolute accuracy of 0.025% and 1° in the V band (Nordsieck, private communication). HPOL spectroscopic data are not calibrated to an absolute flux level due to the non-photometric skies routinely present (Harries et al. 2000) .

[5]IRAF is distributed by the National Optical Astronomy Observatories, which are operated by the Association of Universities for Research in Astronomy, Inc., under contract with the National Science Foundation.

Table 1 provides a log of the observations from both observatories.

3. Results

3.1. Spectroscopic Variability

We now discuss the spectral evolutionary history of V838 Monocerotis from February 5 to March 14. Our observations of V838 Mon from February 5 to February 9, during the onset of the second photometric outburst, indicate an overall shift toward a higher ionization state (Iijima & Della Valle 2002; Morrison et al. 2002) as compared with initial observations (Zwitter & Munari 2002).

Hα shows a strong P-Cygni profile, with electron scattering wings extending at least $\pm$ 1100 km s^{-1} from February 5 to February 8 and about 850 km s^{-1} on February 9, and an average heliocentric blue edge radial velocity of -300 km s^{-1} (see Figure 1). This radial velocity is slightly lower than the terminal velocity of -500 km s^{-1} observed in late January in CaII, BaII, NaI, and LiI lines (Munari et al. 2002b). Goranskii et al. (2002) report that a spectrum on February 5 shows Hα with FWZI = 3100 km s^{-1} and an absorption component at -300 km s^{-1}, which is inconsistent with our findings. The extent of the electron scattering wings strongly depends on accurate continuum placement. We are confident that, within the limits of the SNR of our data, we see a 5 Å "flat" continuum region at each end of the spectral interval containing Hα, hence we are accurately determining the continuum level. The total equivalent width peaked on February 6 (see Table 3), and then began a steady decrease. Equivalent width errors were calculated using $\sigma^2 = N(h_\lambda/SNR)^2(f_*/f_c)$, where N is the number of pixels across a line, h_λ is the dispersion in Å pixel^{-1}, f_* is the flux in the line, f_c is the flux at the continuum, and SNR is the signal to noise ratio (Chalabaev & Maillard 1983).

In early February, all the strong lines exhibited significant line profile variability. In Hα (Figure 1), the emission peak migrated to longer wavelengths with time. The high velocity component of Si II 6347.1Å and 6371.4Å (Figure 2) weakens with time, and the instrinsic component of Na I 5889.95Å and 5895.9Å (Figure 3) also shows variability. Note that since the interstellar Na I components appear to be saturated, they could not fit with gaussians and subtracted to reveal the pure intrinsic component. The low resolution HPOL spectrum (Figure 4) on February 8 clearly depicts the P-Cygni profiles of FeII 4923.9Å, 5018.4Å, 5169.0Å and the CaII infrared triplet 8498.0Å, 8542.1Å, 8662.1Å. Hydrogen Paschen absorption lines at 8438.0Å, 8467.3Å, 8598.4Å, 8750.5Å, 8862.8Å, 9014.9Å, 9229.0Å are observed, as well as HI 10049.4Å, which has a clear P-Cygni profile.

By February 14, the P-Cygni profile of Hα had weakened considerably(Table 3, Figure 1) and its absorption and emission components were approaching equality in strength. The strong electron scattering wings previously observed had disappeared by our February 14 observation. Goranskii et al. (2002) noted that the Hα electron scattering wings had disappeared in their spectrum taken on February 16. These results are consistent with a decreasing excitation level in the circumstellar envelope. A low resolution red HPOL spectrum, obtained on February 13 (Figure 6), reveals two other qualitative changes: the emission components of both the P-Cygni CaII infrared triplet lines and HI 10049.4Å line significantly decreased in strength.

By the end of the third photometric outburst, a significant shift in V838 Mon's spectral characteristics had occurred. Specifically, our spectra on March 11 showed that a second, high velocity absorption component had developed in a few lines. Hα (Figure 1) clearly shows this component, centered at a radial velocity of -200 km s^{-1} with a blue edge radial velocity of -280 km s^{-1}. Figure 2 shows that this feature is also present in the SiII 6347.1Å line, centered at -200 km s^{-1} with a blue edge radial velocity of -260 km s^{-1}, and in the SiII 6371.4Å line, centered at -140 km s^{-1} with a blue edge radial velocity of -190 km s^{-1}. Based upon the radial velocities of these dual absorption features, we identify the enormous P-Cygni profile around 6394Å, seen in Figure 2, as FeI 6393.6Å. A strong P-Cygni profiled line in the vicinity of 6190Å, which we attribute to FeI 6191.6Å, also emerged on March 11 (Figure 5). Figure 1 also reveals new spectroscopic features at 6544.9Å, 6577.2Å, and 6582.5 Å, which we attribute to MgII 6545.9Å and CII 6578.1Å and 6582.9Å. The apparent emergence of both higher excitation lines (CII and MgII) simultaneously with lower excitation lines (FeI) illustrates the complexity of V838 Mon's outburst. In fact, nearly all 9 orders of our spectra show evidence for the emergence of new spectral features on March 11 and March 14. Due to low signal to noise ratios, as well as uncertainties in line blending and profile shapes, we are unable to identify all lines definitively. Since many of these lines are consistent with the rest wavelengths of FeI, NeI, NiI, TiII, MgII, and FeII, and since as noted above we have positively identified two lines of FeI emerging on March 11, these results indicate that V838 Mon began to experience a shift to a lower ionization state. The evidence for spectral evolution that we observed will need to be combined with that of other authors to portray a comprehensive picture of V838 Mon's outbursts.

3.2. Spectropolarimetric Variability

Figures 5-6 illustrate the wavelength dependent polarization of V838 Mon on February 8 and February 13 respectively. The differences between these two observations are

readily apparent. The integrated Johnson R band polarization of the February 8 data is $P = 3.226 \pm 0.004\%$ at a position angle of $149.0 \pm 0.1°$, while the R band polarization of the later observation is $P = 2.667 \pm 0.004\%$ at a position angle of $153.4 \pm 0.1°$. This change strongly suggests the presence of an intrinsic polarization component. Furthermore, the February 8 data are characterized by strongly depolarized emission lines, while the February 13 polarimetric data show no line features. Polarimetric studies of Be stars (Harrington & Collins 1968; Coyne 1976) have found that in contrast to continuum photons, line emission, which predominantly originates in Be circumstellar disks, has a low probability of being scattered. With a few exceptions (McLean & Clarke 1979; Quirrenbach et al. 1997), emission lines should show little to no intrinsic polarization. Thus an intrinsically polarized emission line star should exhibit depolarized emission lines, e.g. a superposition of polarized continuum flux and unpolarized line flux. If one employs a similar argument with the ejecta of V838 Mon, the strongly depolarized emission lines of February 8 may be used to infer the interstellar polarization component (ISP). Similarly, the absence of depolarization effects in the February 13 data suggests that this polarization minima may be primarily attributed to interstellar polarization. As previously noted, the electron scattering wings of Hα disappeared by February 14. Since one expects electron scattering in the ejecta of V838 Mon to be the primary source of any intrinsic polarization, the disappearance of the electron scattering wings is consistent with the hypothesis that the polarization signal observed on February 13 is primarily interstellar in nature.

In order to parametrize the wavelength dependence of the interstellar polarization in the February 13 data, we fitted the empirical Serkowski law (Serkowski et al. 1975), as modified by Wilking et al. (1982) to these data. The resulting ISP parameters are: $P_{max} = 2.746 \pm 0.011\%$, $\lambda_{max} = 5790 \pm 37\AA$, $PA = 153.43 \pm 0.12°$, $\delta PA = 0$, and $K = 0.971$. This fit is overlaid in Figures 5 -6. This Serkowski fit provides a near perfect fit to the February 13 observation; furthermore, it nicely fits the depolarized emission lines in the February 8 observation. We qualitatively crosscheck this claim by using the polarization and extinction relationship, formulated by Serkowski et al. (1975), $3E_{B-V} \leq P_{max} \leq 9E_{B-V}$. Munari et al. (2002b) established a lower limit for the interstellar reddening of $E_{B-V} \sim 0.25$ and suggested that the finding of Zwitter & Munari (2002), $E_{B-V} = 0.80 \pm 0.05$, represents an upper limit. Following the arguments of Munari et al. (2002b), we adopt the midpoint of these values, $E_{B-V} = 0.50$, which bounds the interstellar polarization along the line of sight to V838 Mon by $1.5\% \leq P_{max} \leq 4.5\%$, and thus qualitatively agrees with our ISP determination. Munari et al. (2002b) reported preliminary polarimetry results in which they suggested the ISP is characterized by $P_{max} = 2.6\%$ at 5500 Å at a position angle of $150 \pm 2°$. We are thus confident that our parametrization accurately describes the interstellar polarization component.

We used these Serkowski parameters to remove the ISP component from the February

8 data, as seen in Figure 4, leaving only the intrinsic component. We find the integrated V band intrinsic polarization to be $P = 0.983 \pm 0.012\%$ at a position angle of $127.0 \pm 0.5°$. It is interesting that the intrinsic polarization is clearly not wavelength independent, which one would expect in the case of pure electron scattering. Rather, the polarization gradually increases at wavelengths shortward and longward of $\sim$ 8000Å, which suggests the presence of an absorptive opacity source in V838 Mon's ejecta. A possible Paschen jump, albeit only at a one-sigma detection level, is visible in the raw and intrinsic polarization in Figure 4. Combined with the spectroscopic observations of strong Hα electron scattering wings on February 8, this might suggest a not unlikely speculation that hydrogen is the opacity source (Wood et al. 1996, 1997).

3.3. Distance Estimations

The distance to V838 Mon has yet to be agreed upon. Munari et al. (2002a,b) followed the propagation of V838 Mon's light echo, assuming a spherical distribution of scattering material, to derive a distance of 790 ± 30 pc. Kimeswenger et al. (2002b) used the same technique on a different data set to estimate a distance of 640 to 680 pc. Bond et al. (2002) estimated a distance of 2.5 kpc from HST light echo images; however, it has been suggested that the geometry assumed by these authors is unrealistic (Munari et al. 2002b; Kimeswenger et al. 2002b). More recently, the reported detection of a hot binary companion (Desidera & Munari 2002; Wagner & Starrfield 2002; Munari et al. 2002c) has led Munari et al. (2002c) to suggest a distance of 10-11 kpc, based upon spectrophotometric parallax. We add to the above discussion by considering the distance implied by our spectroscopic and polarimetric observations.

Based upon the assumption that cataclysmic variables contain no intrinsic polarization, Barrett (1996) suggested a rough relationship between polarization and distance. When applied to sources near the Galactic Plane, for distances $\leq$ 1 kpc, this relation is given by $P/d = 3.6\%$ kpc^{-1}. Given our estimate of P_{max} of 2.746%, this would suggest a distance to V838 Mon of 763 pc.

V838 Mon's strong, double interstellar Na I D lines provide a different constraint on the distance. At galactic longitude 217.8°, radial velocities of objects outside the solar circle are positive and increase monotonically with increasing distance from the sun. Thus, the radial velocity of the longer wavelength component provides a lower limit on the distance to V838 Mon. The radial velocities of the two components of the D lines were measured in the spectra of February 5, 6, 8, and 9. For D1 and D2, the means and standard deviations were, respectively, 21.9 ± 0.6, 22.1 ± 0.8, 47.9 ± 0.8, and 47.5 ± 2.8 km s^{-1}, relative to the LSR.

Note that our data are accurate to 2 km s^{-1}, as compared to the IAU velocity standard β Gem, which is constant to better than 0.1 km s^{-1} (Larson et al. 1993).

To read off the distance of the 48 km s^{-1}, further cloud, we used the velocity contour map by Brand & Blitz (1993), which does not assume the velocity field of Galactic rotation to be axisymmetric. The galactic longitude of V838 Mon coincides with an interesting feature in this map, an "island" of high velocities of about 50 km s^{-1} located about 2500 pc from the Sun. We estimate that distances consistent with this velocity map, for a radial velocity of +48 km s^{-1}, lie in the range 2500 ± 300 pc. This estimate constitutes our lower limit on the distance to V838 Mon. Velocities as large as 50 km s^{-1} are not reached again in this direction at heliocentric distances less than 8 kpc. Since this lower limit is greater than 1 kpc, the distance estimation technique used with our polarimetric data is no longer applicable.

4. Discussion

Our spectroscopic data offer both qualitative and quantitative insight into the initial stages of the 2002 outburst. Future modeling efforts can be constrained by the equivalent width variability of the lines presented. Furthermore, the complex line profile variability and evolution of various species and ionization stages of lines presented in this paper should also provide constraints on future attempts to explain this outburst.

In spite of our sparse polarimetric data set, these observations clearly demonstrate that the ejecta of V838 Monocerotis deviated significantly from a spherical geometry. We note the similarity between our observations and those of Bjorkman et al. (1994), who found Nova Cygni 1992 to have an intrinsic polarization signal during the initial stages of outburst. These authors suggest the intrinsic polarization during this initial stage was caused by electron scattering in a slightly flattened spheroidal shell. As the shell expanded, the electron scattering optical depth decreased, hence the intrinsic polarization declined. A similar interpretation could be applied to V838 Mon. The electron scattering wings around Hα were sizable on February 5, but had clearly weakened by February 9 and disappeared by February 14. Coupled with our discovery of an intrinsic polarization component present on February 8 but gone by February 13, this picture of an expanding, flattened spheroidal shell could provide a viable explanation of the intrinsic polarization observed during the 2002 outburst.

Finally, we consider the implications of these observations for future studies of this object. Munari et al. (2002b) and Kimeswenger et al. (2002b) discuss different classifications of V838 Mon, including a nova outburst, a post-AGB star, a M31-Red type variable, and a

V4332 Sgr type variable: both suggest that V838 Mon is most similar to a V4332 Sgr type variable. As described above, we suggest that the geometry of the outburst, as probed by polarimetry, might be similar to that of a nova outburst. This suggests that the geometry of V4332 Sgr's, V838 Mon's, and nova outbursts might be similar. It would be worthwhile to measure the polarization of V4332 Sgr today, to verify that like V838 Mon, it has no intrinsic polarization at a time long after outburst. Furthermore, we suggest that polarimetric observations immediately following the outbursts of all future V4332 Sgr type variables be made. Such observations would provide an ideal testbed to correlate the geometry of each outburst, and hence help to identify the true nature of these unique objects.

We would like to thank Dr. Kenneth H. Nordsieck for providing access to the HPOL spectropolarimeter. We also thank Brian Babler for his help with various aspects of HPOL data reduction and management. We thank the anonymous referee for helping to improve this paper. Support for observational research at Ritter Observatory has been provided by the University of Toledo, with technical support provided by R.J. Burmeister. K.S.B. is a Cottrell Scholar of the Research Corporation, and gratefully acknowledges their support. This research has made use of the SIMBAD database operated at CDS, Strasbourg, France, and the NASA ADS system.

REFERENCES

Banerjee, D.P.K. & Ashok, N.M. 2002, A&A, 395, 161

Barrett, P. 1996, PASP, 108, 412

Bjorkman, K.S., Johansen, K.A., Nordsieck, K.H., Gallagher, J.S., & Barger, A.J. 1994, ApJ, 425, 247

Bond, H.E., Panagia, N., Sparks, W.B., Starrfield, S.G., Wagner, R.M., & Henden, A.A. 2002, IAU Circ., 7943

Brand, J. & Blitz, L. 1993, A&A, 275, 67

Brown, N.J. et al. 2002, IAU Circ., 7785

Chalabaev, A. & Maillard, J.P. 1983, A&A, 127, 279

Coyne, G.V. 1976, A&A, 49, 89

Desidera, S. & Munari, U. 2002, IAU Circ., 7982

Goranskii, V.P., Kusakin, A.V., Metlova, N.V., Shugarov, S.Yu, Barsukova, E.A., & Borisov, N.V. 2002, Astron. Lett., 28, 691

Harries, T.J., Babler, B.L., & Fox, G.K. 2000, A&A, 361, 273

Harrington, J.P. & Collins, G.W.II 1968, ApJ, 151, 1051

Henden, A., Munari, U., & Schwartz M. IAU Circ., 7859

Iijima, T. & Della Valle M. 2002, IAU Circ., 7822

Kaeufl, J.U. Locurto, G., Kerber, F., & Heijligers, B. 2002, IAU Circ., 7831

Kato T., Yamaoka, H., & Kiyota, S. 2002, IAU Circ., 7786

Kimeswenger, S., Lederle, C., & Schmeja, S. 2002a, IAU Circ., 7816

Kimeswenger, S., Lederle, C., Schmeja, S., & Armsdorfer, B. 2002b, MNRAS, 336, L43

Larson, A.M., Irwin, A.W., Yang, S.L.S., Goodenough, C., Walker, G.A.H., Walker, A.R., & Bohlender, D.A. 1993, PASP, 105, 825

McLean, I.S. & Clarke, D. 1979, MNRAS, 186, 245

Morrison, N.D., Knauth, D.C., Mulliss, C.L., & Lee, W. 1997, PASP, 109, 676

Morrison, N.D., Bjorkman, K.S., Miroshnichenko, A., & Wisniewski, J.P. 2002, IAU Circ., 7829

Munari, U., Henden, A., Corradi, R.L.M., & Zwitter, T. 2002a, in "Classical Nova Explosions", Sitges (Spain) 20-24 May 2002, M. Hernanz & J. Jose ed., AIP Conf. Proc. 637, 52

Munari, U. et al. 2002b, A&ALett, 389, L51

Munari, U., Desidera, S., & Henden, A. 2002c, IAU Circ., 8005

Nook, M. 1990, Ph.D. dissertation, The University of Wisconsin-Madison

Nordsieck, K.H. & Harris, W. 1996, in ASP Conf. Ser. 97, Polarimetry of the Interstellar Medium, ed. W. G. Roberge & D. C. B. Whittet (San Francisco: ASP), 100

Quirrenbach, A. et al. 1997, ApJ, 479, 477

Rauch, T., Kerber, F., & Van Wyk, F. 2002, IAU Circ., 7886

Serkowski, K., Mathewson, D.S., & Ford, V.L. 1975, ApJ, 196, 261

Wagner, R.M. & Starrfield, S.G. 2002, IAU Circ., 7992

Wilking, B.A., Lebofsky, M.J., & Rieke, G.H. 1982, AJ, 87, 695

Wolff, M.J., Nordsieck, K.H., & Nook, M.A. 1996, AJ, 111, 856

Wood, K., Bjorkman, J.E., Whitney, B., & Code, A. 1996, ApJ, 461, 847

Wood, K., Bjorkman, K.S., & Bjorkman, J.E. 1997, ApJ, 477, 926

Zwitter, T. & Munari, U. 2002 IAU Circ., 7812

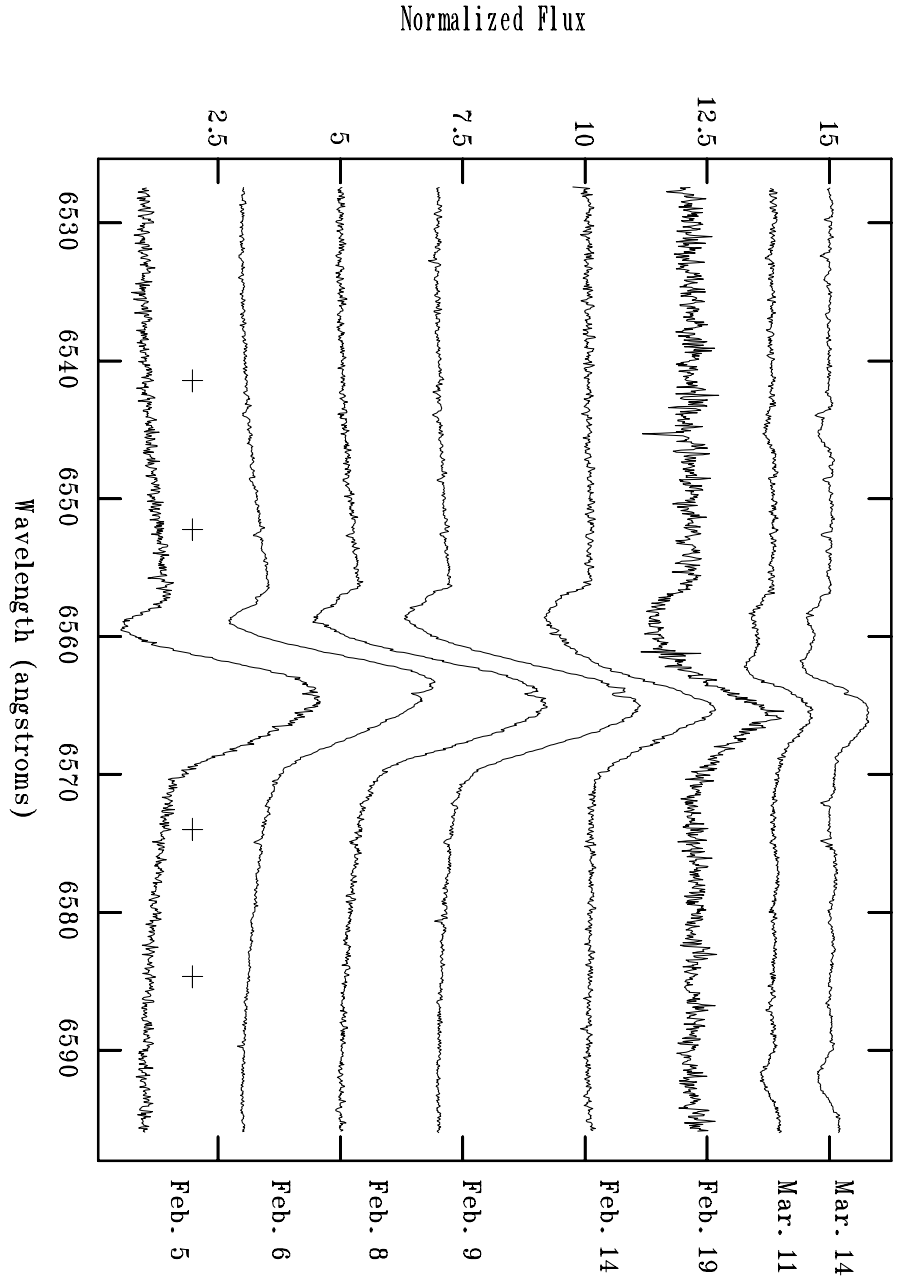

Fig. 1.— Hα line profiles sorted chronologically. From shorter to longer wavelengths, the tick marks denote -1000 km s^{-1}, -500 km s^{-1}, 500 km s^{-1}, and 1000 km s^{-1}.

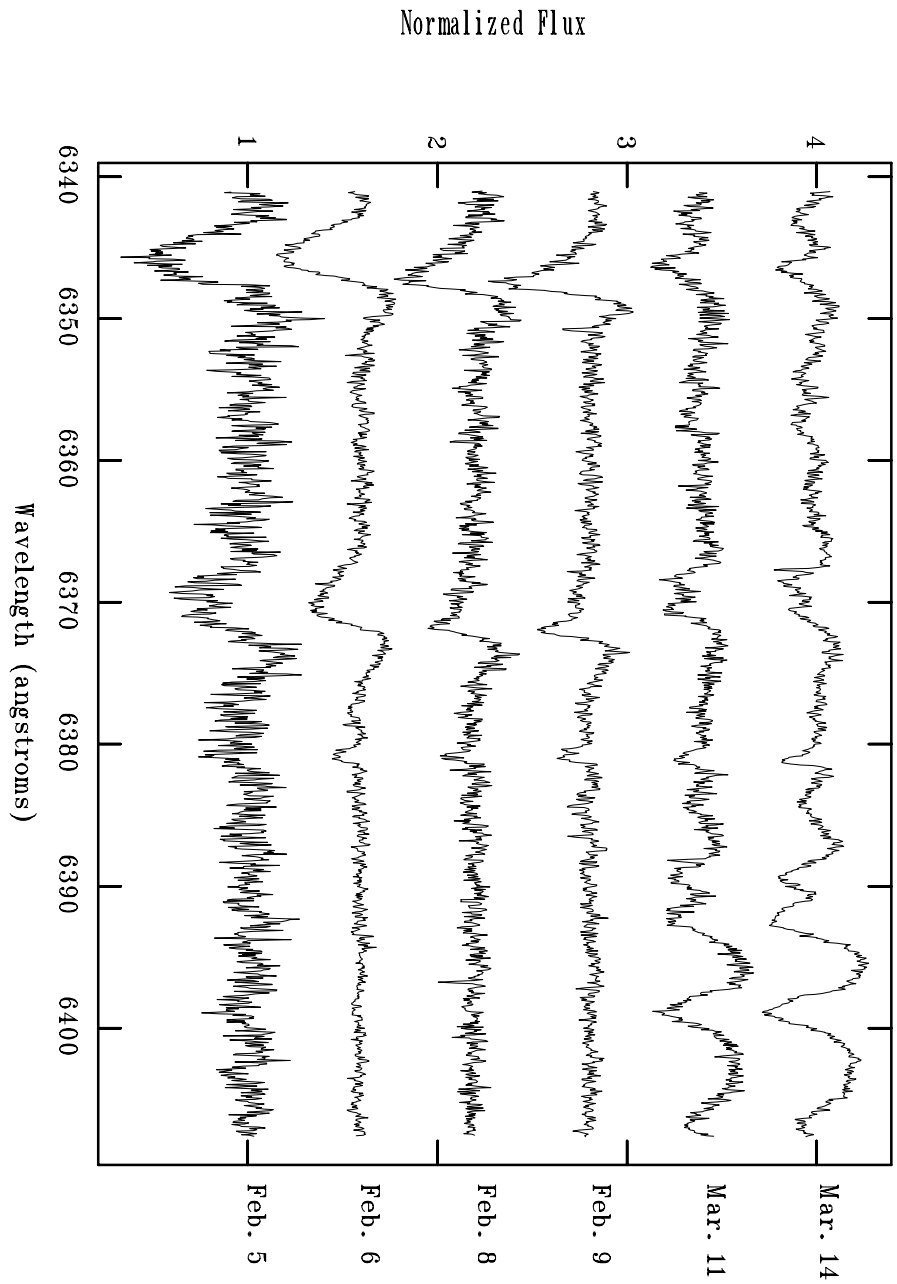

Fig. 2.— SiII 6347.1Å and 6371.4Å line profiles sorted chronologically.

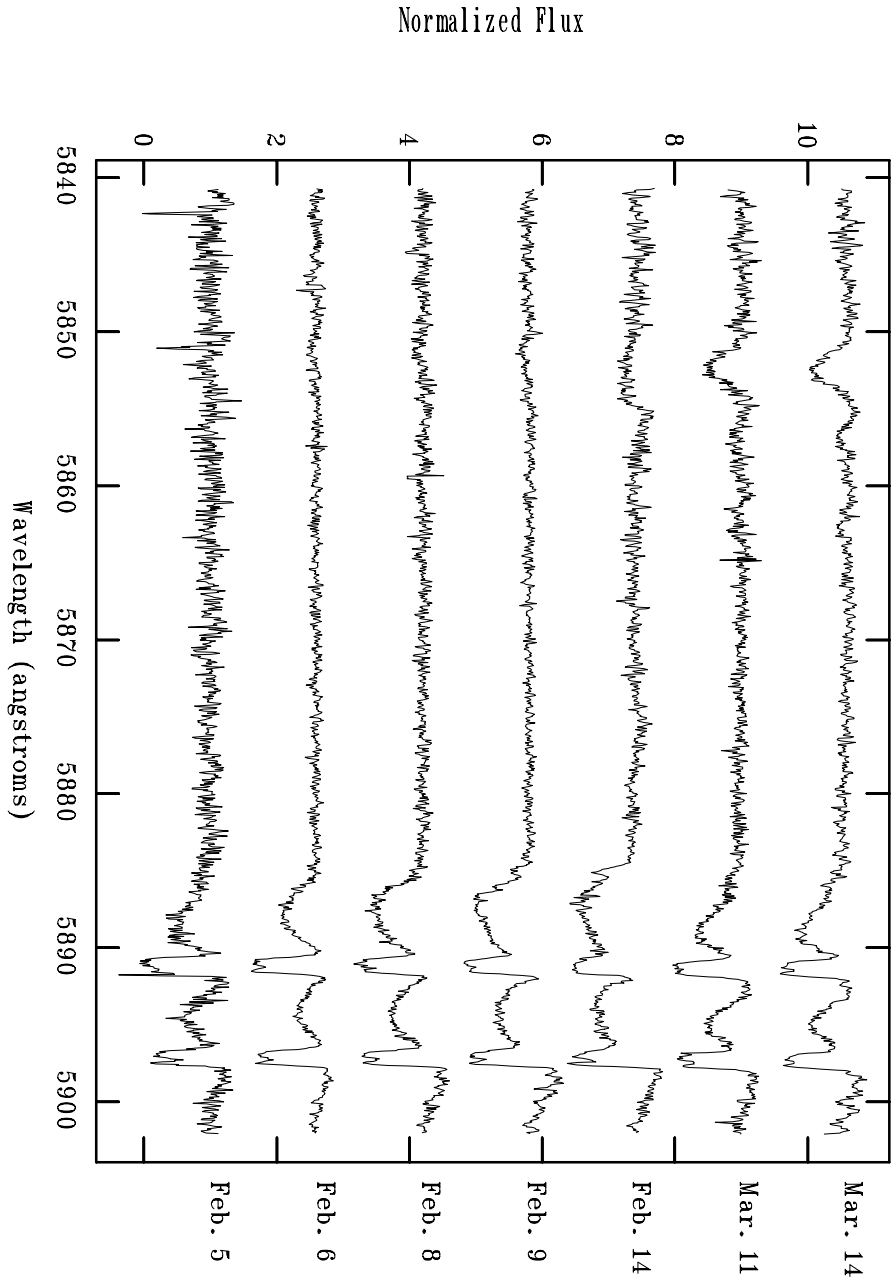

Fig. 3.— NaI 5889.95Å and 5895.92Å line profiles sorted chronologically. Note that the narrow interstellar line components are superimposed on the intrinsic components. As discussed in section 3.1, the saturation of the interstellar components prevents the isolation of the intrinsic components.

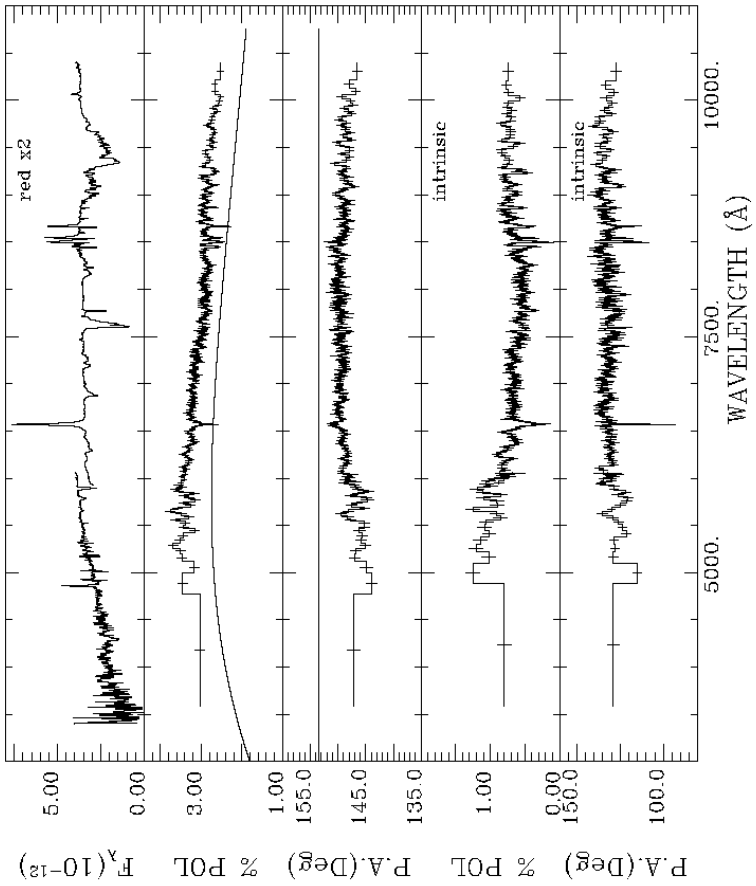

Fig. 4.— HPOL spectropolarimetry from February 8. The upper panel shows the flux, in units of ergs cm^{-2} s^{-1} $\AA^{-1}$, with the red data magnified by a factor of 2. The next two lower panels display the total polarization and position angle, where the red data, e.g. 6000 - 10500Å, are binned to a constant error of 0.075% and blue data, e.g. 3200 -6000Å, are binned to a constant error of 0.12%. Overplotted is the derived Serkowski interstellar polarization component, whose parameters are given by: $P_{max} = 2.746 \pm 0.011\%$, $\lambda_{max} = 5790 \pm 37\AA$, $PA = 153.43 \pm 0.12°$, $\delta PA = 0$, and $K = 0.971$. The bottom two panels show the intrinsic polarization and position angle, binned to constant errors of 0.07% and 0.10% for the red and blue data respectively. The wavelength dependence of the intrinsic polarization is not representative of pure electron scattering; rather, it implies the presence of an opacity source such as hydrogen.

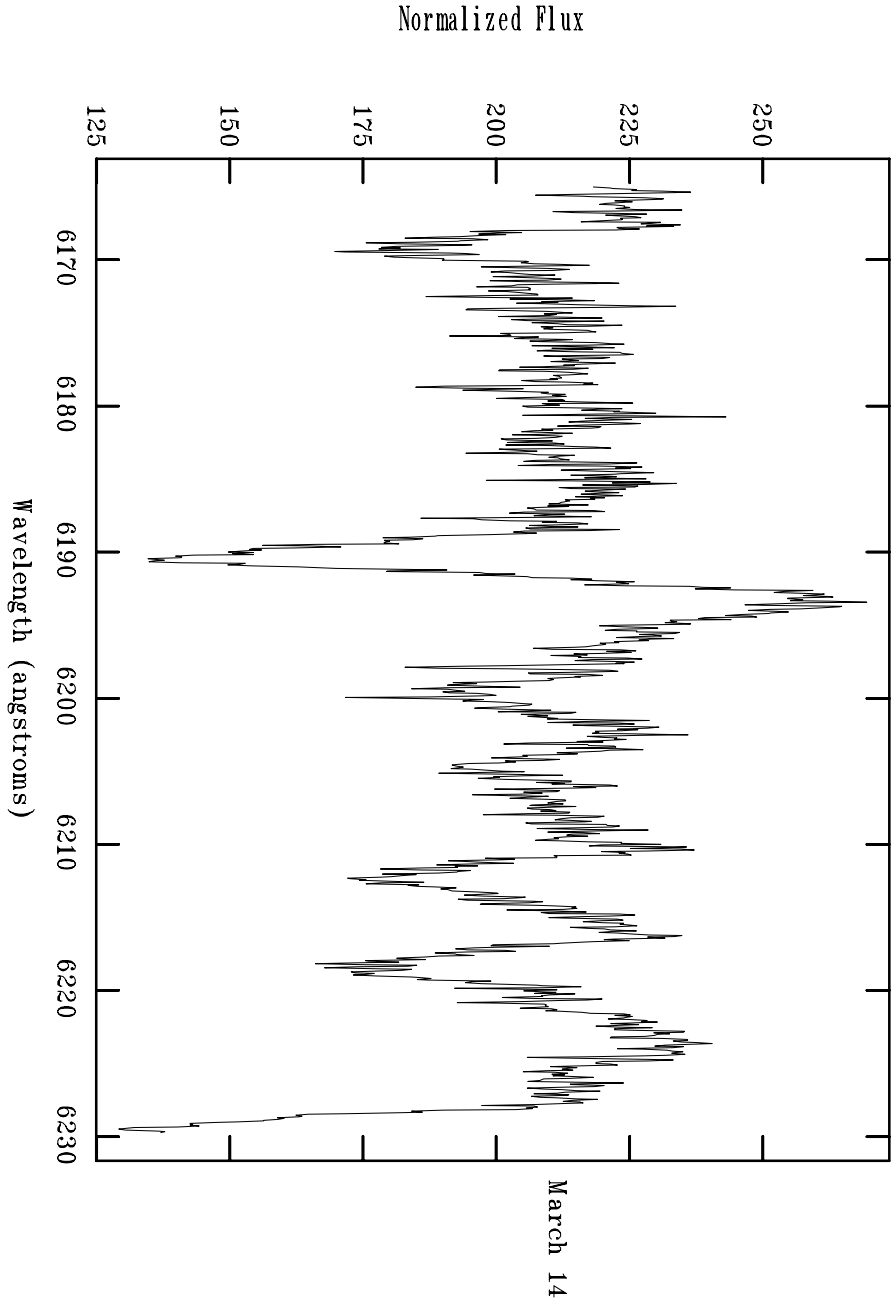

Fig. 5.— A strong P-Cygni profile, attributed to FeI 6191.6Å, is shown in a non-continuum normalized spectrum from March 14.

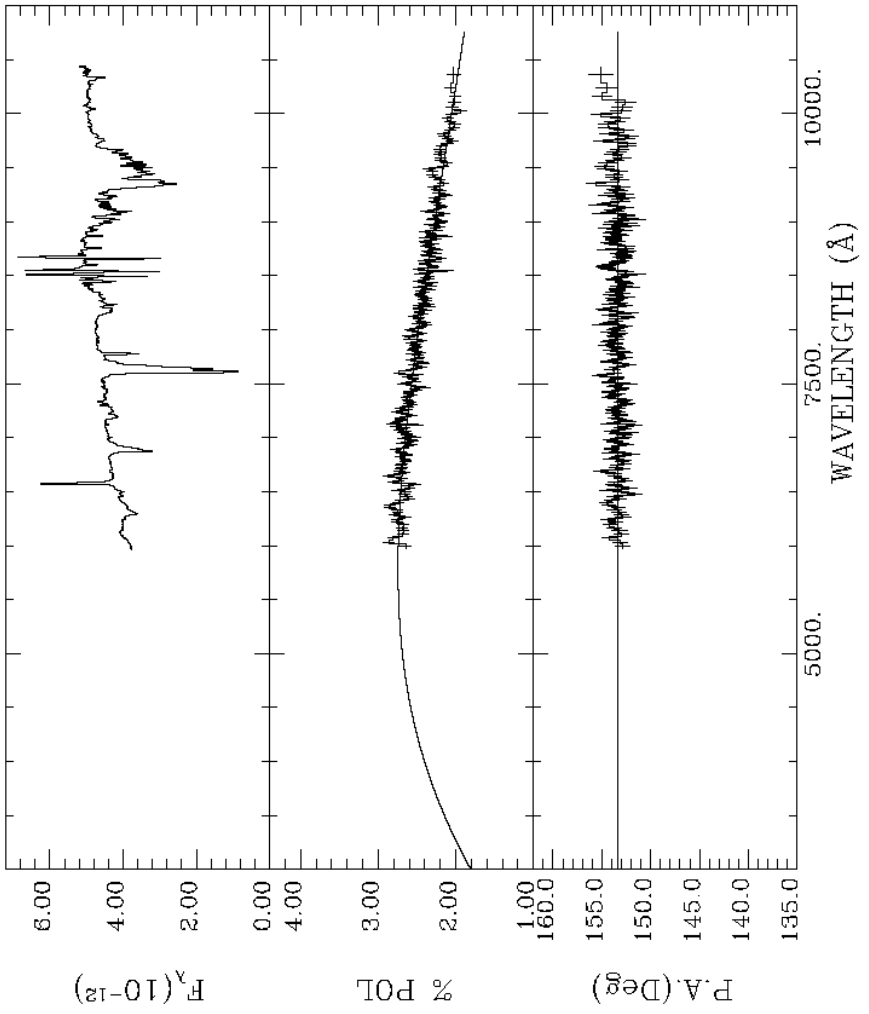

Fig. 6.— HPOL spectropolarimetry from February 13. The upper panel shows the flux, in units of ergs cm^{-2} s^{-1}Å^{-1}. The lower two panels give the total polarization and position angle, binned to a constant error of 0.074%. The fitted interstellar polarization component is given by the solid line. The intrinsic polarization which was present on 8 February has clearly disappeared by February 13.

Table 1:

UT Date, 2002	MJD	Observatory	SNR: Hα	SNR: Si II	SNR: Fe I	SNR: Na I
February 5	2452310.7	Rit	24	22	···	18
February 6	2452311.7	Rit	84	68	···	42
February 8	2452313.6	Rit	48	42	···	32
February 8	2452313.7	HPOL	···	···	···	···
February 9	2452314.7	Rit	66	64	···	46
February 13	2452318.8	HPOL	···	···	···	···
February 14	2452319.7	Rit	42	···	···	28
February 19	2452324.6	Rit	14	···	···	···
March 11	2452344.6	Rit	60	64	···	32
March 14	2452347.6	Rit	104	84	78	34

Note. — Summary of observations. Rit denotes Ritter spectroscopy and HPOL denotes HPOL spectropolarimetry. Multiple observations during one night were coadded, using standard IRAF techniques, to increase the SNR. The Modified Julian Dates listed correspond to the midpoint of the observations for a specific night. The signal to noise ratios cited are the signal to noise ratios per resolution element, calculated in line free regions of the spectrum.

Table 2:

Line	MJD								
	2452310.6	2452311.6	2452313.6	2452314.6	2452318.7	2452319.6	2452324.6	2452344.6	2452347.6
Hβ	...	...	e[1]	...	...	...	...	...	...
FeII 4923.9Å	...	...	p[1]	...	...	...	...	...	...
FeII 5018.4Å	...	...	p[1]	...	...	...	...	...	...
FeII 5169.0Å	...	...	p[1]	...	...	...	...	...	...
FeII 5316.2Å	p	p	p[1]	p	...	p?	...	a	a
NaI 5889.95Å	p	p	p	p	...	p	...	p	p
NaI 5895.9Å	p	p	p	p	...	p	...	p	p
FeI 6191.6Å	...	...	...	...	...	...	...	p	p
SiII 6347Å	p	p	p	p	...	...	...	p[2]	p[2]
SiII 6371Å	p	p	p	p	...	...	...	p[2]	p[2]
NII 6380Å	a	a	a	a	...	...	...	a	a
FeI 6393.6Å	...	...	...	...	...	...	...	p[2]	p[2]
Hα	p	p	p	p	p[1]	p	p	p[2]	p[2]
CII 6576Å	...	...	...	...	...	...	...	e	e
CII 6583Å	...	...	...	...	...	...	...	e	e
CaII 8498Å	...	...	p[1]	...	p[1]	...	...	...	...
CaII 8542Å	...	...	p[1]	...	p[1]	...	...	...	...
CaII 8662Å	...	...	p[1]	...	p[1]	...	...	...	...
Paschen	...	...	a[1]	...	a[1]	...	...	...	...
HI 10049.4Å	...	...	p?[1]	...	p?[1]	...	...	...	...

Note. — Observed spectral lines and their general characteristics (p = P Cygni profile, a = absorption, e = emission). [1] denotes line identification via low resolution HPOL spectropolarimetry. [2] denotes multiple absorption components observed.

Table 3:

Line	MJD							
	2452310.6	2452311.6	2452313.6	2452314.6	2452319.6	2452324.6	2452344.6	2452347.6
Hα (total)	-29.15 ±0.75	-34.22 ±0.25	-33.42 ±0.43	-27.88 ±0.26	-9.01 ±0.15	-3.40 ±0.26	-0.66 ±0.03	-0.73 ±0.02
SiII 6347Å (abs)	1.49 ±0.06	1.22 ±0.02	0.80 ±0.02	0.81 ±0.02	···	···	0.53 ±0.01	0.45 ±0.01
SiII 6347Å (em)	-0.28 ±0.02	-0.36 ±0.01	-0.35 ±0.01	-0.29 ±0.01	···	···	-0.11 ±0.01	-0.12 ±0.01
SiII 6371Å (abs)	0.90 ±0.05	0.81 ±0.02	0.48 ±0.02	0.45 ±0.01	···	···	0.43 ±0.01	0.37 ±0.01
SiII 6371Å (em)	-0.31 ±0.02	-0.30 ±0.01	-0.25 ±0.01	-0.25 ±0.01	···	···	-0.25 ±0.01	-0.23 ±0.01
NII 6380Å	0.19 ±0.01	0.15 ±0.01	0.13 ±0.01	0.13 ±0.01	···	···	0.12 ±0.01	0.13 ±0.01
FeII 5316.2Å (abs)	1.98 ±0.16	1.51 ±0.07	1.65 ±0.10	1.42 ±0.06	1.03 ±0.09	···	0.77 ±0.08	0.55 ±0.04
FeII 5316.2Å (em)	-2.27 ±0.20	-2.39 ±0.11	-2.76 ±0.17	-3.01 ±0.10	-2.87 ±0.20	···	-0.55 ±0.09	-0.63 ±0.06

Note. — Equivalent width, in Å, of selected spectral lines for the 8 nights of Ritter observations. Except for Hα all measurements were made on spectra smoothed with a boxcar function of size 3.